ELSEVIER

Remote Sensing of Environment 79 (2002) 72–83

Remote Sensing of Environment

www.elsevier.com/locate/rse

Design and analysis of numerical experiments to compare four canopy reflectance models

C. Bacour[a,*], S. Jacquemoud[a], Y. Tourbier[b], M. Dechambre[c], J.-P. Frangi[a]

[a]*Laboratoire Environnement et Développement, Université Paris 7 — Denis Diderot, Case 7071, 2 place Jussieu, 75251 Paris Cedex 05, France*
[b]*Renault — Direction de la Recherche, 1 avenue du Golf, 78288 Guyancourt Cedex, France*
[c]*Centre d'Etude des Environnements Terrestre et Planétaires, 10–12 avenue de l'Europe, 78140 Vélizy, France*

Received 10 July 2000; received in revised form 27 April 2001; accepted 8 May 2001

Abstract

A method designed to study the relative effects of the input parameters of any model has been investigated with canopy reflectance (CR) models. Traditionally, sensitivity analyses are performed by changing one input parameter at a time. Such an approach is limited because it lacks strategy. A promising alternative is in the use of design of experiments, a statistical method that allows defining a structured and restricted number of simulations for which all input parameters vary simultaneously. This approach is especially helpful in multidimensional parameter spaces. It is demonstrated using four 1D radiative transfer models that are compared in direct mode. These models are combinations of the PROSPECT leaf optical properties model with the four CR models, SAIL (Scattering and Arbitrarily Inclined Leaves), KUUSK, IAPI, and NADI (New Advanced DIscrete model). The sensitivity studies were conducted in the visible/near-infrared on the following parameters: the leaf structure (N), the chlorophyll-a and -b content (C_{ab}), the leaf area index (LAI), the mean leaf inclination angle (θ_l), the hot spot (s_l), and the soil brightness (α_{soil}). We compared simulated reflectances for a given set of measurement geometries and two wavebands of the POLDER (Polarization and Directionality of the Earth's Reflectances) spaceborne instrument. The relative effects of the biophysical parameters are assessed as well as their contribution to reflectance, allowing us to rank the most influential ones. Their interactions were also studied from the perspective of improving inversion procedures. Globally, the four models agree well in terms of computed reflectances and parameter effects, nevertheless with some discrepancies due to the implementation of different leaf angle distribution (LAD) functions.

1. Introduction

Even though vegetation covers only a fraction of the Earth surface, the knowledge of its state and evolution over time is of primary interest as it represents the major part of the biomass involved in the carbon and water cycles, and because it controls energy exchanges between the surface and the atmosphere. The question of the carbon sink is for instance, a burning issue for the global change community. The development of optical remote sensing has permitted a better understanding of those processes from a local to a global scale. In particular, the way solar radiation and vegetation interact reveals biome functioning since the analysis of the reflectance allows the retrieval of major canopy characteristics. Among all of the extraction methods, those relying on physically based models that calculate top-of-canopy reflectances have proved to be a promising alternative to estimate vegetation biophysical parameters. However, the existence of many bidirectional reflectance models with different levels of complexity makes the choice particularly difficult for scientific or operational use. Consequently, the need to compare these models is legitimate. This can be achieved either with regard to the top-of-canopy reflectance they simulate or to their representation of the radiation field within the medium.

When a new model emerges in the literature, it is generally validated against experimental data but increasingly by comparison with another 1D model (Kuusk, 1995a) or a 3D model that is assumed to better predict the canopy BRDF (Gobron, Pinty, Verstraete, & Govaerts, 1997; Iaquinta & Pinty, 1994; Kuusk, 1995a; Kuusk, Andrieu, Chelle, & Aries, 1997), since field experiments are complex and expensive to organize. The agreement between the computed bidirectional reflectances is nevertheless only

* Corresponding author. Tel.: +33-1-44-27-60-47; fax: +33-1-44-27-81-46.
E-mail address: bacour@ccr.jussieu.fr (C. Bacour).

0034-4257/02/$ – see front matter
PII: S0034-4257(01)00240-1

evaluated for a limited number of simulations: two to eight bidirectional reflectances are typically computed for two spectral bands (visible and near-infrared) with some input parameters arbitrarily chosen. Goel (1988), Myneni et al. (1995), and more recently Jacquemoud, Bacour, Poilve, and Frangi (2000), performed simulations with the aim of assessing discrepancies between several canopy reflectance (CR) models. A more ambitious project involving the international community, and named RAMI (RAdiation transfer Model Intercomparison), has been initiated by the Joint Research Centre during the Second International Workshop on Multiangular Measurements and Models in Ispra, Italy (Pinty et al., 2001). The goal of this program was to provide benchmark plant canopies for the development and testing of models, both in direct and inverse mode. Apart from RAMI, most investigations to compare models on the basis of their outputs (reflectances) have involved a limited number of simulations, often without any consideration for the inner behavior of the models with respect to their input parameters.

In optical remote sensing, sensitivity analyses (i) determine the response of a numerical model (the simulated spectral and/or bidirectional reflectance) to variations of its input parameters (chlorophyll content, leaf area index, etc.) and (ii) verify that the model behavior agrees with expectations. They characterize a model in direct mode and help to improve the biophysical parameter estimation in inversion, once the prevailing effects have been determined. Typically, two kinds of sensitivity analyses are practiced: sensitivity of the response with respect to the parameters and sensitivity of the parameters themselves. In most instances, it stands for a series of simulations that, from a fixed initial baseline of input parameters, consists in changing each one sequentially (Iaquinta, 1995; Jacquemoud, 1993). This mode of evaluation has serious limitations. First, because the choice of the initial parameter set is often arbitrary and decided without rules and second, because a possible interaction between the parameters may be neglected (Saltelli, 1999). This can be bypassed by defining a discrete number of values for each parameter and by performing simulations for all the combinations. Consider, for instance, a model with six input parameters, each with seven values distributed within their range of variation. A complete study over the parameter space might be time consuming to test since it would lead to $7^6 = 117{,}649$ simulations! Asner (1998) and Privette, Myneni, Emery, and Hall (1996) have a slightly different approach. They investigated the variation of reflectance when each parameter is changed by 10% from a baseline reflectance distribution. Privette et al. defined directionally averaged sensitivity indices for some input parameters of the DISORD model, depending on the root mean square error (RMSE) between the baseline and the new reflectance distributions, in the red and the near-infrared at three solar zenith angles. Asner studied the sensitivity of SAIL (Scattering and Arbitrarily Inclined Leaves) by performing a principal components analysis on the RMSE, for 220 AVIRIS wavebands. As a result, he could appreciate the relative contribution of some structural variables. In order to quantify the sensitivity of a CR model to its parameters and their correlation, Combal, Oshchepkov, Sinyuk, and Isaka (2000) recently proposed a statistical method. Nonetheless, these methods still face the abovementioned problems.

In this study, we propose to quantify the influence of input parameters on CR models when varied simultaneously, for limited and better-structured computer runs. Experimental designs recently emerged in the field of remote sensing with Dechambre and Le Gac (2001), who applied this method as a way to validate a microwave backscattering model. This technique, developed by Fisher (1925), was very popular in agriculture and in manufacturing industry to conceive and improve production processes. By analogy with laboratory experiments, calculations with numerical models are referred to as numerical experiments. The use of numerical experiments is recent and applies to expanding research fields: they can be used to fit statistically complex and nonlinear models with large parameter spaces (Bowman, Sacks, & Chang, 1993) or to identify the most influential parameters of physical systems (e.g., Church & Lynch, 1998; Spuzic, Zec, Abhary, Ghomashchi, & Reid, 1997). Moreover, a full investigation of the interaction between parameters is made possible.

The intercomparison of four CR models is first conducted on the reflectance computed for a single set of input parameters. The planning of numerical experiment is then applied to generalize the comparison. It is used to build a reflectance database corresponding to a wider range of canopies. This database is exploited to compare the models according to the impact and to the contribution of their input parameters to the reflectance.

2. Methods

2.1. Models

Among many bidirectional CR models available, the SAIL (Verhoef, 1984, 1985), KUUSK (Kuusk, 1995a), IAPI (Iaquinta & Pinty, 1994), and NADI (New Advanced DIscrete model, Gobron et al., 1997) models can be coupled with PROSPECT (Jacquemoud et al., 1996, 2000) to take into account the spectral dimension of the signal. The combined models have been renamed PROSAIL, PROKUUSK, PROSIAPI, and PRONADI, respectively. These models differ in the level of approximation of the radiative transfer equation and in the description of the canopy architecture. SAIL and KUUSK both derive from the Kubelka–Munk theory to describe the scattering and extinction of four upward/downward fluxes within the canopy; IAPI and NADI (“one-angle” versions) rather consist in solving analytically and numerically the different scattering orders of the radiative transfer equation. A preliminary stage was to make them coherent so as they accept the same input

variables: the leaf area index (LAI), the mean leaf inclination angle (θ_l), the hot spot parameter (s_l), the soil reflectance spectrum (ρ_s, assumed Lambertian), and a soil brightness parameter (α_{soil}). The latter controls the reflectance levels of a given soil, depending on whether it is wet or dry. It ranges from 0.5 to 2. In each model, s_l is defined as the ratio between the average length of a single leaf and the canopy height. Still, the description of the phenomenon in SAIL and KUUSK differs from IAPI and NADI: in the first two, it is based on Kuusk's (1985) approach, whereas IAPI and NADI follow the approach of Verstraete, Pinty, and Dickinson (1990). In SAIL, IAPI, and NADI, the leaf angle distribution (LAD) is ellipsoidal and characterized by a mean leaf inclination angle (θ_l) (Campbell, 1990). We could not implement it in KUUSK where the original elliptical LAD is also used to analytically approximate the phase and *G* functions. The two LADs are unfortunately not strictly comparable: the ellipsoidal one considers a distribution of leaf inclinations proportional to the surface area of an ellipsoid (Campbell, 1986), whereas the elliptical one assumes that the leaf normal distribution is proportional to its radius. The elliptical distribution depends on two parameters: eln, related to the eccentricity χ of the ellipsoid, and the leaf modal inclination (θ_m). Both distributions coincide well in the spherical case. Finally, the specular effects due to reflection on the leaf surface are removed in PROKUUSK. The version of PROSPECT used here is the last one that requires the leaf structure parameter (*N*), the chlorophyll-*a* and -*b* content (C_{ab}, $\mu g\ cm^{-2}$), the equivalent water thickness (C_w, $g\ cm^{-2}$ or cm), and the dry matter content (C_m, $g\ cm^{-2}$) to simulate leaf reflectance and transmittance spectra in the optical domain (Jacquemoud et al., 2000).

A first attempt to compare the models has been achieved by simulating the spectral and bidirectional reflectances of a standard plant canopy: $N=1.5$, $C_{ab}=35\ \mu g\ cm^{-2}$, $C_w=0.015$ cm, $C_m=0.01\ g\ cm^{-2}$, LAI = 2, spherical LAD ($\theta_l=57°$, eln = 0, and $\theta_m=0°$ for PROKUUSK), $s_l=0.25$, and $\alpha_{soil}=1$. The Markov parameter (λ_z) of the PROKUUSK model is set to 1 so that the canopy structure corresponds to the Poisson stand geometry assumed in the other models. CRs have been calculated in the red (670 nm) and near-infrared (865 nm) bands of the POLDER (Polarization and Directionality of the Earth's Reflectances) spaceborne instrument (Deschamps et al., 1994) and for $\theta_v=\pm49.7°$, $\pm43.9°$, $\pm37.2°$, $\pm29.3°$, $\pm20.3°$, $\pm10.4°$, and 0°, assuming a sun zenith angle of 30°. Fig. 1a shows a good agreement between the four spectral reflectances simulated both at nadir ($\theta_v=0°$) and near the hot spot direction ($\theta_v=29.3°$), considering the various mathematical formalisms of these models. The differences are the largest in the near-infrared where multiple scattering prevails; they are lower in the visible due to the strong absorption of light by chlorophyll. The reflectances simulated at 670 and 865 nm as a function of the viewing zenith angle also show a good superimposition both in the forward and backward directions (Fig. 1b). Those results reflect the consistency of the models for a *particular* canopy. The comparison of models was then expanded to various kinds of artificial canopies by use of the design of experiments.

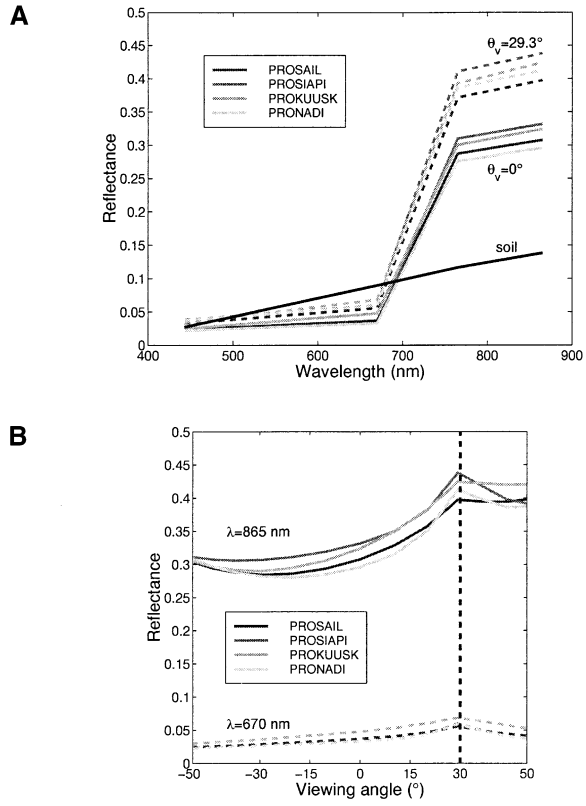

Fig. 1. Canopy (A) spectral reflectance simulated by PROSAIL, PROSIAPI, PROKUUSK, and PRONADI at nadir ($\theta_v=0°$) and near the hot spot direction ($\theta_v=29.3°$) and shape of a standard soil reflectance spectrum; (B) bidirectional reflectance simulated by the same models at 670 and 865 nm (the dashed line indicates the sun direction).

2.2. Design of experiments

Experimental designs aim at maximizing the information that can be extracted from a limited number of simulations (Box, Hunter, & Hunter, 1978). The matrix of runs is generated statistically to explore the parameter space. It gathers all the simulations (*experiments*), for which the input parameters are varied in a structured pattern. A column of this matrix corresponds to the values (*levels*) taken by a particular parameter (*factor*) along the experiments. A line is a simulation to realize. Each one thus differs from another by the combination of the factors' levels. We used the design of experiments to (i) determine the simulation set for the study of six parameters and (ii) quantify the effects of these parameters to the reflectance. Because a complete design, covering all possible combinations of the parameter levels, would be too demanding in computer resources, we directed our choice towards a *fractional* table of experiments, an orthogonal subset of the complete table, in order to reduce the number of simulations. An exhaustive

description of the method is given by Benoist, Tourbier, and Germain-Tourbier (1994).

The effects of the input parameters of a given CR model are the estimated coefficients $\hat{\alpha}_i$ of the empirical model that linearly connects the response to the p variables ν_i ($i=1, \ldots, p$) explaining the reflectance, with respect to a constant term I (Eq. (1)):

$$\rho_k = I + \sum_{i=1}^{p} \hat{\alpha}_i \nu_{ik} \varepsilon_k \quad (1)$$

where ρ_k is the reflectance computed for the numerical experience k, the value of the constant term I is set to the mean value of the experiment results: $I=\bar{\rho}$, and the residue ε_k expresses the difference between the linear model and the physical CR model. Estimating the regression model coefficients enables to quantify the influence of the different factors to the computed reflectances. The $\hat{\alpha}_j$ coefficients are assessed so as to minimize the least square criterion on the residues ε. If the level m of a factor ν_p appears n_m times in the table (in the waveband, λ, and for the zenith viewing angle, θ_v), the mean of the results is (Eq. (2)):

$$\bar{\rho}_{\nu_p,m}(\lambda,\theta_v) = \frac{\sum \rho_{\nu_p,m}(\lambda,\theta_v)}{n_m} \quad (2)$$

when ν_p is at the level m. The corresponding effect of ν_p, $\hat{\alpha}_{\nu_p,m}(\lambda,\theta_v)$ can be then expressed as (Eq. (3)):

$$\hat{\alpha}_{\nu_p,m}(\lambda,\theta_v) = \bar{\rho}_{\nu_p,m}(\lambda,\theta_v) - \bar{\rho}(\lambda,\theta_v) \quad (3)$$

where $\bar{\rho}(\lambda,\theta_v)$ is the general averaged reflectance over the N numerical experiments, in the waveband (λ) and for the viewing angle (θ_v). Because the influence of each parameter is evaluated against $\bar{\rho}(\lambda,\theta_v)$, which is specific to each model, the normalized effects will be expressed as a percentage in order to cast off the model dependence (Eq. (4)):

$$E_{\nu_p,m}(\lambda,\theta_v) = \frac{\hat{\alpha}_{\nu_p,m}(\lambda,\theta_v)}{\bar{\rho}(\lambda,\theta_v)} \times 100 \quad (4)$$

The method is first illustrated with three simple and complete designs used to assess the LAI effect. Computations are conducted with PROSAIL (viewing at nadir, 670, and 865 nm). In the first complete table, 10 simulations are obtained by varying the LAI 10 times within the range [0–7]. The other two tables allow simultaneous study of two parameters of 10 levels each, i.e., 10^2 numerical experiments: LAI plus C_{ab}, and LAI plus θ_l, C_{ab}, and θ_l being defined within [1–80] and [5–85], respectively (Fig. 2). A positive (respectively, negative) effect indicates that, for the corresponding level of the parameter, the reflectance increases (respectively, decreases) by this percentage, in relation to the mean reflectance. For instance, when LAI is equal to 0.6, from the first experimental design and at 670 nm, the computed reflectance is up to 71% higher than the mean reflectance; when LAI is equal to 6.4, the reflectance is 14.5% lower than the mean one. Therefore, the slope of

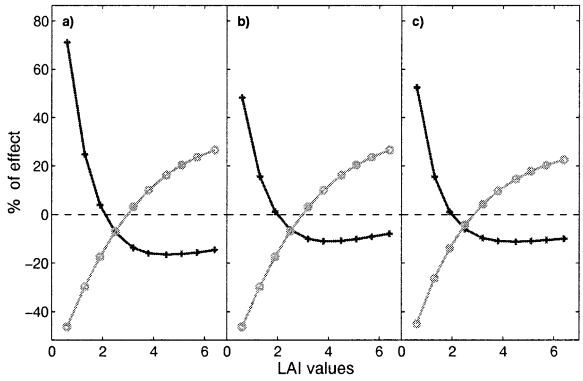

Fig. 2. Effect of LAI on CRs computed with PROSAIL at nadir, at 670 nm (+) and 865 nm (○), when the experimental design is built to study (a) LAI alone, (b) LAI and C_{ab}, and (c) LAI and θ_l, according to Eq. (4). The mean set of parameters is: $N=1.5$, $C_{ab}=35$ μg cm^{-2}, $C_w=0.015$ cm, $C_m=0.010$ g cm^{-2}, $\theta_l=57°$, $s_l=0.25$, $\alpha_{soil}=1$, horizontal visibility = 50 km, and $\theta_s=30°$.

the curve representing the parameter effect is instructive on the sensitivity of that parameter: a positive (respectively, negative) slope means that increasing the value of the given parameter, leads to increase (respectively, decrease) the reflectance. Also, the sharper the slope is, the more sensitive the reflectance is to variations of the considered parameter. Fig. 2 clearly shows the nonlinearity of the LAI effect and its spectral dependence. At 865 nm, an increase of LAI induces an increase of reflectance; the trend is opposite at 670 nm, as noticed earlier by Goel (1988) or Clevers and Verhoef (1991), for instance. Beyond 4, the slope of the LAI effect is positive at both wavebands but the reflectance is weakly sensitive, especially in the red as compared to the near-infrared. The different experimental conditions show some slight differences according to the experimental matrix and to the number of simulations involved. Indeed, even if the curves are similar, some discrepancies on magnitude are observed: for a LAI equal to 0.6, the effect at 670 nm is +71% when the simulations are conducted on LAI alone, +48% on LAI and C_{ab}, and +52% on LAI and θ_l. These differences should be attributed to inherent residues. The accuracy of the effect coefficients mainly depends on the number of simulations rather than on the simulations themselves, because they are determined rigorously: as it is a statistically based method, the error in the effect determination decreases as the number of simulations involved increases. This preliminary study shows that the method is a useful tool to study the parameter sensitivity of a particular model.

2.3. Simulations

The intercomparison of the four CR models is now carried out by means of experimental designs. CRs have been calculated for the configuration of the spaceborne POLDER instrument: 4 wavebands (443, 670, 765, and 865 nm) and 13 viewing angles (±49.7°, ±43.9°, ±37.2°,

Table 1
Values of the input parameters used for the simulations

Parameter	Unit	Column of the $L_{343}7^{57}$ design	Range of variation	Levels
LAI	$m^2\ m^{-2}$	1	0–7	0.4, 1.4, 2.5, 3.5, 4.6, 5.6, 6.7
C_{ab}	$\mu g\ cm^{-2}$	17	1–80	5, 17, 29, 41, 52, 64, 76
θ_l	degrees (°)	26	5–85	9, 21, 33, 45, 57, 69, 81
s_l		2	0.01–1	0.06, 0.21, 0.36, 0.51, 0.65, 0.80, 0.95
α_{soil}		32	0.5–2	0.57, 0.80, 1.02, 1.25, 1.48, 1.70, 1.93
N		9	1–2.5	1.1, 1.3, 1.5, 1.8, 2.0, 2.2, 2.4

$\pm 29.3°$, $\pm 20.3°$, $\pm 10.4°$, 0°) where positive values indicate the sun azimuthal direction. In total, 52 reflectances per numerical experiment are available. Data from computer runs are collected using a *Hyper Graeco Latin Geometric* sampling scheme (Benoist et al., 1994) where all factors have the same number of levels. The experiment table used is named $L_{343}7^{57}$: it is designed to study up to 57 factors with seven levels in 343 simulations. Because this plan is not complete (a complete one would include 7^{57} experiments), columns of some actions are *aliases* of others (that is, they are linearly combined), and then are unusable to conduct a sensitivity study. For those reasons, only six independent parameters are considered with this table. The choice of seven levels for each single parameter is driven by the nonlinear behavior of LAI and C_{ab}, for instance, and is a compromise because more levels would greatly increase the number of simulations. The values taken by the parameters are summarized in Table 1: the lowest (highest) values correspond to the lower (upper) bounds of the ranges of variation, increased (decreased) by 5%. The other levels are regularly spaced between these two bounds. The values of eln and θ_m are derived from θ_l and χ values, according to the ellipsoidal distribution formalism ($\theta_m = 90°$ if $0 \leq \chi \leq 1$ and $\theta_m = 0°$ if $1 < \chi < \infty$), and are given in Table 2. Note that the elliptical distribution departs from other distributions in extreme cases (planophile and erectophile canopies) (Kuusk, 1995b). From now on, eln and θ_m will be referred as to θ_l. The fixed input parameters are: $C_w = 0.015$ cm and $C_m = 0.010$ g cm^{-2}. As the matrix of runs contains 343 simulations, a total of 17,836 ($343 \times 4 \times 13$) reflectances have been computed. The effect of the variables is assessed for each of the 13 view angles.

Table 2
Correspondence between θ_l and eln–θ_m values

θ_l (°)	eln	θ_m (°)
9	5.113	0
21	3.577	0
33	2.499	0
45	1.479	0
57	0	0
69	1.884	90
81	3.872	90

3. Results

3.1. Comparison between the computed reflectances

The consistency of the four models was tested in the principal and perpendicular planes. Because no reference model for the reflectance was available, we decided to represent PROKUUSK, PROSIAPI, and PRONADI, as a function of PROSAIL because the latter is the oldest and the most widespread model (Fig. 3). Over all the simulations, PROSAIL and PRONADI are the closest models (Table 3). The discrepancies are of the same order in the principal and in the perpendicular plane. The agreement between PROSAIL and PROSIAPI is slightly lower but still one can observe a low RMSE and a good correlation. PROKUUSK and PROSAIL show the strongest differences. Note that the last two models take into account diffuse radiation contrary to PROSIAPI and PRONADI. This may explain, to a small extent, some of the reflectance gaps.

Fig. 4 shows the directional gaps between PROSAIL and the other three models in both planes, over the 343 simulations. These results strengthen the previous observations. Namely, the main dissimilarities occur in the near-infrared (the models differ in the way multiple scattering is accounted for) whereas they are weak in the visible. PRONADI provides the closest results to PROSAIL. PROKUUSK, PROSIAPI, and PRONADI mainly differ from PROSAIL around nadir. Note that even though PROSIAPI and PRONADI have a similar representation for the hot spot parameter, the RMSE between PROSAIL and PRONADI in this direction is smaller at 765 and 865 nm, whereas a peak of increasing RMSE is observed with PROSIAPI. In the perpendicular plane, the RMSE values are symmetrical with respect to the nadir viewing direction, which was expected (the models are built so that the BRDF is symmetrical with respect to the principal plane).

3.2. PROSAIL sensitivity

Before going further into the model intercomparison, let us focus on how the results of experimental designs may be informative about the sensitivity of the input parameters for a given model. Fig. 5 shows the effects of

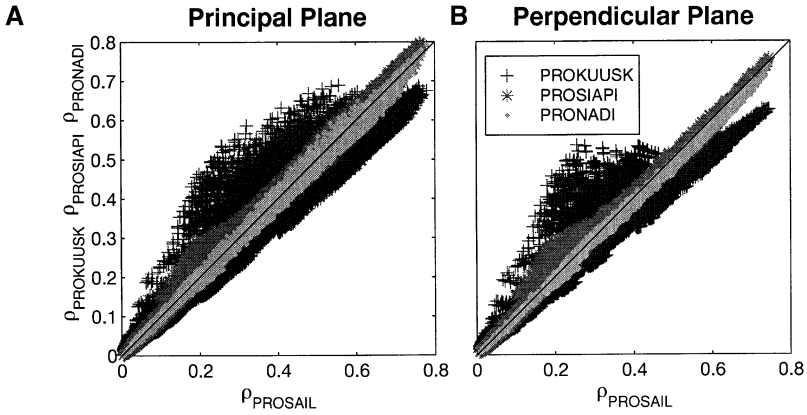

Fig. 3. Comparison between PROKUUSK/PROSIAPI/PRONADI and PROSAIL in (A) the principal plane and (B) the perpendicular plane. The 17,836 reflectances result from the experimental design of Table 1.

the six parameters (N, C_{ab}, LAI, θ_l, s_l, and α_{soil}) to the reflectance computed by PROSAIL over the 343 simulations at 443, 670, 765, and 865 nm. These results indicate which parameters are spectrally and directionally predominant. In the visible, the leaf chlorophyll concentration is the prevailing factor that controls the reflectance; in the near-infrared, it is the LAI and the mean leaf inclination angle. There is a small effect of C_{ab} at 765 and 865 nm, whereas chlorophylls do not absorb light after 760 nm. This could be attributed to the limited number of experiments from which the parameter effects were drawn (for a given level, the effect of a parameter is determined from 49 different simulations) and considered as a quantification of the error in the effect assessment. Furthermore, increasing C_{ab} leads to an exponential-like decrease in its effect, as expected. Apart from the inherent residues, the results obtained with the complete experimental design and discussed earlier are retrieved. Fig. 5 points out the importance of the mean leaf inclination angle: after C_{ab}, it is the most influential factor in the visible. The negative slope indicates that increasing θ_l from a planophile to an erectophile canopy globally induces a decrease of reflectance: a departure from horizontal leaves causes the photons to travel deeper within the canopy, i.e., the signal is more attenuated (Asner, 1998; Myneni, Ross, & Asrar, 1989). The contribution of s_l is the smallest around the retrosolar direction. Finally, the effects of N are level with α_{soil} and their variation is quasi-linear within their respective range of variation. These observations can be extended to PROKUUSK, PROSIAPI, and PRONADI, despite some differences that will be described in the following.

Table 3
Correlation coefficients (R) and RMSE between the reflectances computed by the models, taken two by two, over the whole set of values

	PROKUUSK		PROSIAPI		PRONADI	
	pr	pe	pr	pe	pr	pe
PROSAIL						
R	.968	.973	.998	.998	.999	1
RMSE	.0553	.0514	.0151	.0126	.0126	.0123
PROKUUSK						
R	1	1	.975	.979	.968	.972
RMSE	0	0	.0508	.0457	.0532	.0480
PROSIAPI						
R			1	1	.998	.998
RMSE			0	0	.0163	.0162

For each comparison between two models: the first column corresponds to the principal plane (pr) and the second one to the perpendicular plane (pe).

3.3. Comparison between the models

PROSAIL, PROKUUSK, PROSIAPI, and PRONADI are now compared on the basis of their sensitivity to C_{ab}, LAI, and θ_l for simulations performed in the principal plane at 670 and 865 nm (Fig. 6). The influence of ancillary phenomena like diffuse radiation is negligible in the following. The main differences between the four CR models

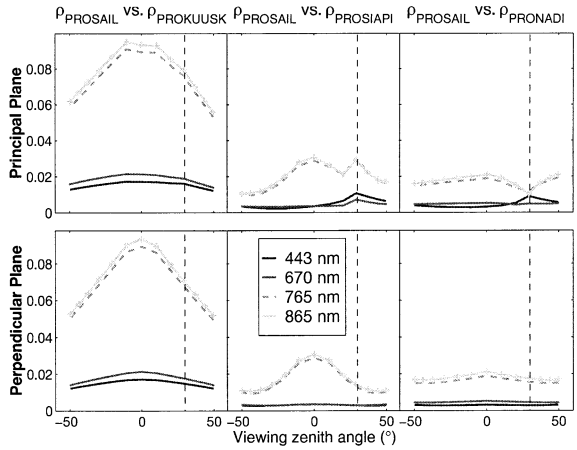

Fig. 4. RMSE between PROSAIL and PROKUUSK, PROSIAPI, and PRONADI, respectively, in the principal (up) and the perpendicular (down) planes, for the four POLDER wavebands.

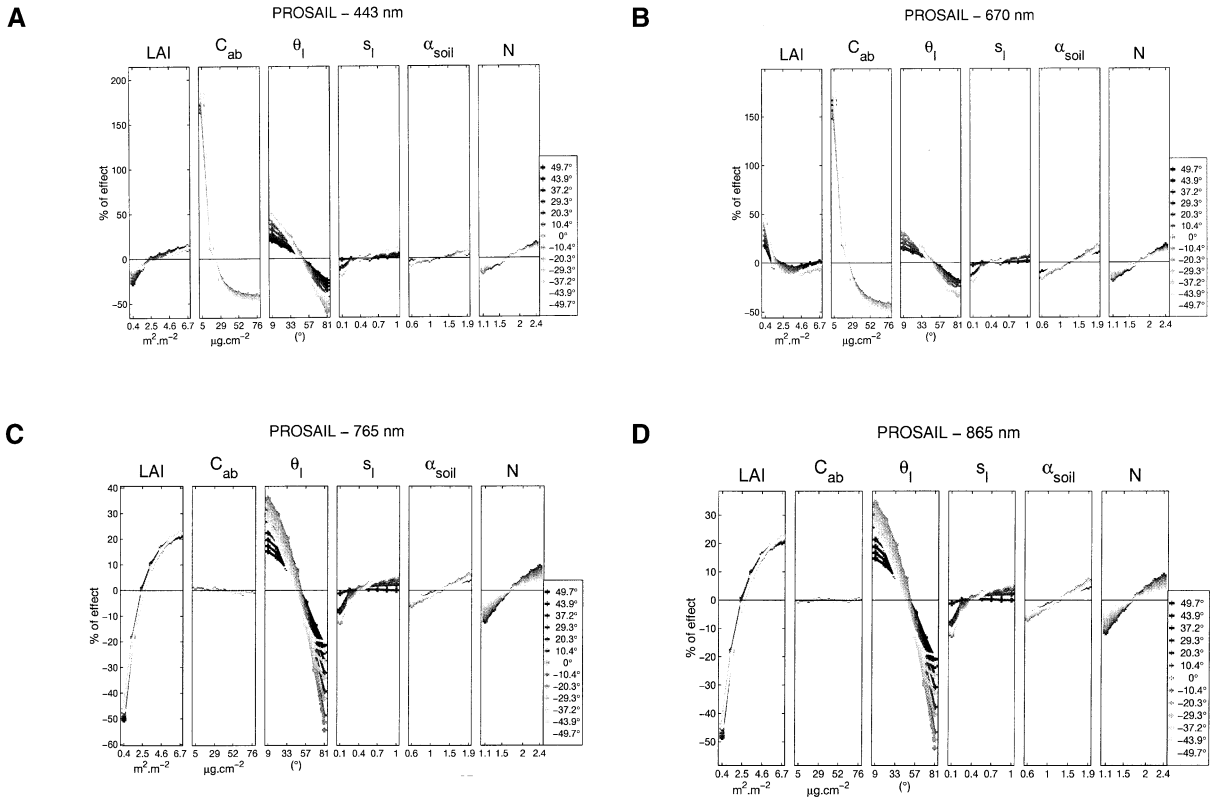

Fig. 5. Effects of N, C_{ab}, LAI, θ_l, s_l, and α_{soil} on the reflectance computed by PROSAIL at (A) 443, (B) 670, (C) 765, and (D) 865 nm for the 13 viewing angles (the nadir view angle is a dashed line).

are conspicuous by the magnitude of the effects of the parameters on the reflectance, whereas the shapes of the curves are often similar. The models are coherent with regard to C_{ab}, which is not surprising since the chlorophyll absorption is accounted for by the same model, PROSPECT. The same behavior can be noted for LAI both at 670 and 865 nm (less than 5% difference in magnitude). LAI influence at 670 nm is the weakest in the hot spot direction, with an amplitude below 10% for most values of this parameter, whereas the forward direction shows the highest influence (backward direction at 865 nm) with an amplitude over 30%. For that particular viewing direction, in the visible, the slope of LAI effect is negative for all values of the LAI, whereas it becomes positive after 4 for the other viewing configurations. The effect of the leaf inclination angle parameter exhibits the strongest discrepancies between the models (Fig. 6C). This was partly expected because the LADs are different as abovementioned. The analytical approximations used in PROKUUSK for the computation of the G and phase functions, simplify and speed up that model, but also cause divergences from PROSAIL (Kuusk, 1995a). The gaps observed in Fig. 6C are then due to these approximations rather than to different LADs. As a consequence, the effect of θ_l in PROKUUSK is strongly attenuated as compared to PROSAIL, PROSIAPI, or PRONADI. Furthermore, whereas the decrease of the θ_l effects is quasi-linear for the last ones, PROKUUSK diverges between 57° and 81°. Finally, note that the general shapes and magnitude of s_l effects are similar for the four models (results not shown).

In order to determine and quantify which parameters are responsible for the discrepancies between the models, let us consider them two by two. The index that characterizes these gaps, attributable to different effect representation is:

$$C\nu_p = \sum_{\lambda} \sum_{\theta_v} \mathrm{RMSE}\nu_p(\lambda, \theta_v)$$

with $\mathrm{RMSE}\nu_p(\lambda,\theta_v)$

$$= \sqrt{\frac{1}{n_\nu} \sum_{1 \le m \le n_\nu} \left[\frac{\hat{\alpha} \bmod 1_{\nu_p,m}(\lambda, \theta_v)}{\bar{\rho} \bmod 1(\lambda, \theta_v)} - \frac{\hat{\alpha} \bmod 2_{\nu_p,m}(\lambda, \theta_v)}{\bar{\rho} \bmod 2(\lambda, \theta_v)} \right]^2}$$

The indices are expressed in percent such as $C\nu_p = 100 \times c\nu_p / \sum_{\nu_p} c\nu_p$ and are gathered in Table 4.

The mean leaf inclination angle parameter displays the highest disparities between the models, even when the latter have the same LAD. This highlights the previous observations concerning the implementation of functions involving

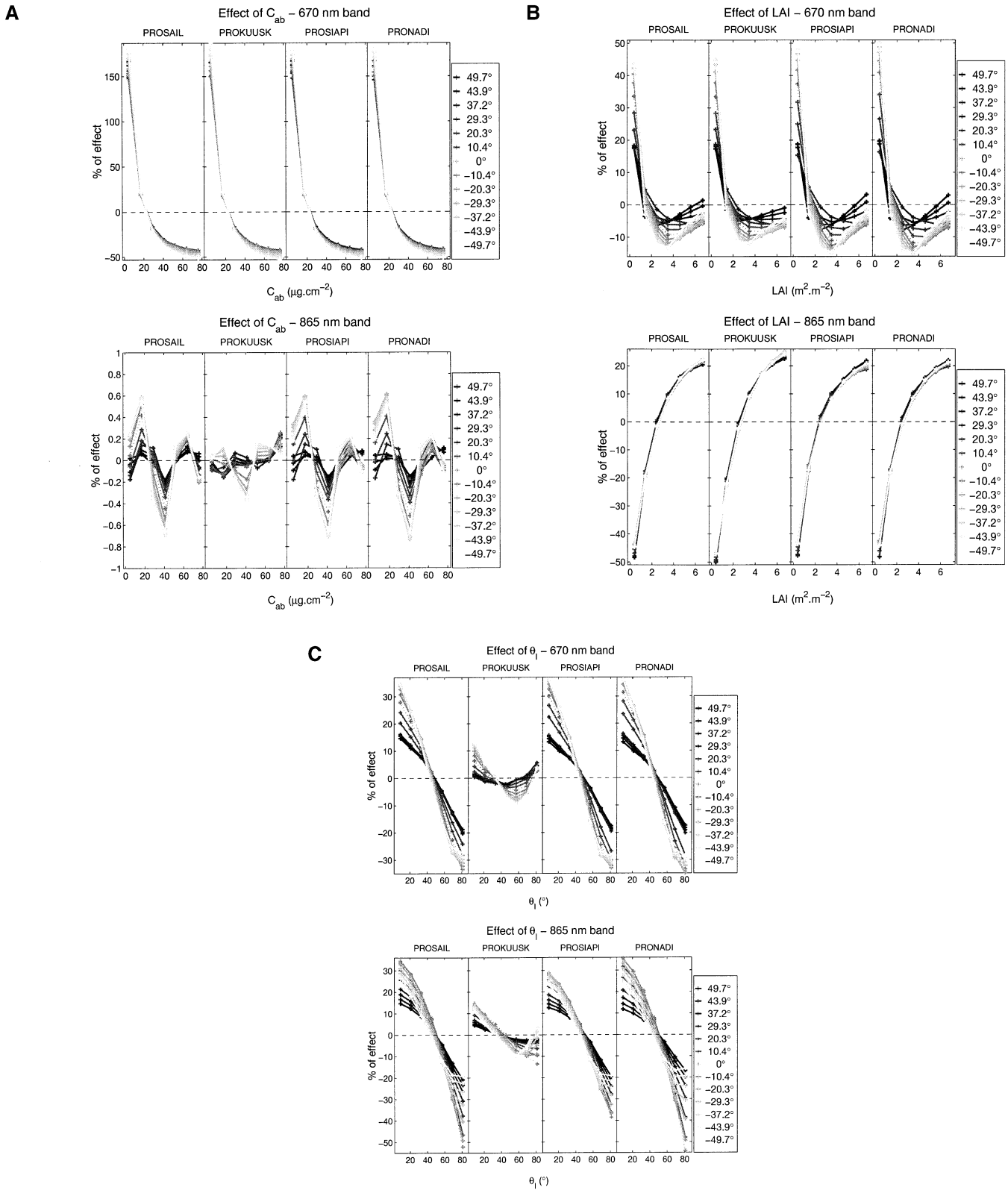

Fig. 6. Effects of (A) C_{ab}, (B) LAI, and (C) θ_l, at 670 and 865 nm, and for the 13 viewing angles (the nadir view angle is a dashed line). For PROKUUSK, the effect of the elliptical leaf angle inclination parameters, eln and θ_m, is represented in relation to the corresponding ellipsoidal θ_l value.

Table 4
Gap indices for parameter effect representation between the four models considered two by two

	PROKUUSK	PROSIAPI	PRONADI
PROSAIL			
LAI	7	20	21
s_l	3	27	**34**
N	3	8	5
C_{ab}	5	9	7
θ_l	**76**	**32**	30
α_{soil}	6	4	3
PROKUUSK			
LAI		11	10
s_l		8	8
N		5	3
C_{ab}		5	5
θ_l		**66**	**69**
α_{soil}		5	5
PROSIAPI			
LAI			18
s_l			5
N			13
C_{ab}			13
θ_l			**46**
α_{soil}			5

In bold are the results that cause the main divergence for each model intercomparison.

the LAD. The main causes of divergences between PROSAIL/PROSIAPI and PROSAIL/PRONADI are due to θ_l and s_l, and are of the same importance. The lowest indices are found for the PROSPECT parameters N and C_{ab}, and for the soil brightness parameter α_{soil}.

3.4. Relative contribution of the factors

An easiest way to form the most influential parameters into a hierarchy is achieved by considering the relative contribution of each factor to the reflectance. For each viewing direction and each waveband, such a contribution index characterizes the contribution of each parameter to the output's variance. It is expressed in percent and evaluated as follows (Eq. (5)):

$$C(\lambda,\theta_\nu)=\frac{\mathrm{SQ}(\nu_p(\lambda,\theta_\nu))}{\mathrm{SQG}(\rho(\lambda,\theta_\nu))}\times 100$$

$$=\frac{\frac{N}{n_\nu}\sum\limits_{1\le m\le n_\nu}\left[\hat{\alpha}_{\nu_p,m}(\lambda,\theta_\nu)\right]^2}{\sum\limits_{1\le k\le N}\left[\rho_k(\lambda,\theta_\nu)-\bar{\rho}(\lambda,\theta_\nu)\right]^2}\times 100 \qquad (5)$$

where n_ν is the number of levels taken by each factor ($n_\nu=7$). Fig. 7 represents the contribution of each factor for the four models at 670 and 865 nm, in the principal plane, with respect to the view angle. Note that the sum of contributions for each factor, in each viewing geometry, is lower than 100% due to the residues and to the fact that no interaction is taken into account so far.

Fig. 7 shows the directional influence of the parameters from an original viewpoint. The chlorophyll content (670 nm) and the LAI (865 nm) most strongly affect the reflectance at high view angles due to larger path lengths within the canopy. Note that these contributions are slightly lower in the forward direction. The contribution of θ_l is symmetrical in relation to the one of LAI, with greater influence in the forward direction. It reaches its highest at nadir where the probability of gap fractions through the entire canopy reaches its maximum with respect to the viewing direction, and is the most sensitive to the leaf orientation (Kimes, 1984). For PROKUUSK, the C_{ab} contribution is a little higher than for the other models but still coherent; on the other hand, θ_l plays a lower role for the same abovementioned reasons. The hot spot parameter contribution is minimal in the retrosolar direction. Indeed, s_l governs the shape of the bidirectional reflectance, whereas the maximum reflectance in that particular direction is the same for different s_l values. Both in the red and near-infrared, the leaf structure parameter contribution increases from high forward to high backward view angles. Fig. 7 also emphasizes the former observations upon the parameters influence hierarchy, similar for each CR model. In the visible, it clearly appears that the chlorophyll content is the major factor affecting the reflectance, followed by the canopy structural parameters. In the near-infrared, the reflectance is principally governed by the LAI and the mean leaf inclination

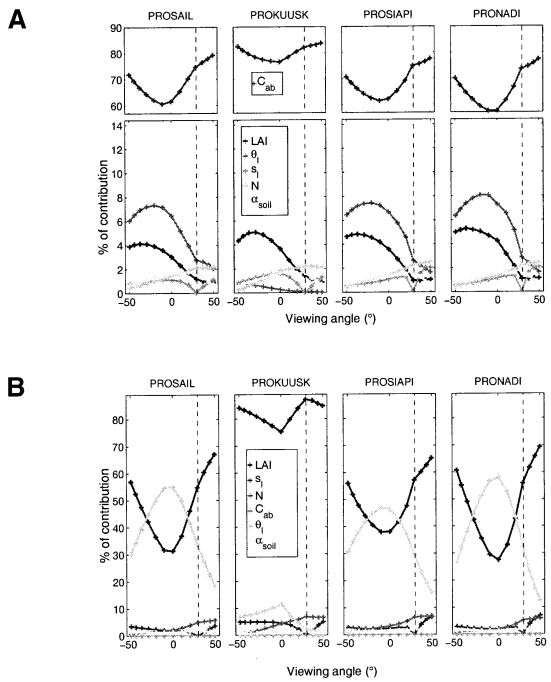

Fig. 7. Compared contribution of LAI, C_{ab}, θ_l, s_l, α_{soil}, and N as a function of the viewing zenith angle at (A) 670 and (B) 865 nm (the dashed line indicates the sun direction).

angle, depending on the view angle, followed by N, s_l, and α_{soil}. To sum up, PROSAIL, PROSIAPI, and PRONADI exhibit similar relative contributions of their parameters, spectrally and directionally.

3.5. Interaction between the parameters

Besides these effects, the design of the experiments allows to quantify a very interesting issue, i.e., the interactions between two input parameters within the radiative transfer models. This notion implies that the influence to the response of the first one depends on the value of the second. The interaction effect between two parameters A (level m) and B (level n) is calculated as follows (Eq. (6)):

$$\hat{\alpha}_{A_mB_n}(\lambda,\theta_v) = \bar{\rho}_{A_mB_n}(\lambda,\theta_v) - \bar{\rho}(\lambda,\theta_v) - \hat{\alpha}_{A,m}(\lambda,\theta_v) - \hat{\alpha}_{B,n}(\lambda,\theta_v) \quad (6)$$

and the contribution index is computed after Eq. (5) with Eq. (7):

$$SQ(I_{A,B}(\lambda,\theta_v)) = \frac{N}{n_A n_B} \sum_{1\le m\le n_A} \sum_{1\le n\le n_B} [\hat{\alpha}_{A_mB_n}(\lambda,\theta_v)]^2 \quad (7)$$

The way the experimental array is built allows study of the interactions, spectrally and directionally, between LAI and C_{ab}, LAI and θ_l, as well as LAI and α_{soil} (Fig. 8).

The results show that some interactions may have a greater impact on the reflectance than some parameters alone: at 670 nm and over all the viewing directions, the averaged contribution of LAI is 2.7% whereas the averaged contribution of LAI–C_{ab} is 6.2% for PROSAIL, even though LAI was the third most influential factor at this waveband. LAI–C_{ab} interaction is the most significant interaction in the visible. For PROSAIL, PROSIAPI, and PRONADI, it is minimal at nadir and maximal in the hot spot direction. From high view angles, the contribution of this interaction increases quasi-linearly until the retrosolar direction is reached for PROKUUSK. This model exhibits the highest results for LAI–C_{ab}, counterbalanced by lower effects of LAI–θ_l and LAI–α_{soil}. Once again, the coherence of PROSAIL, PROSIAPI, and PRONADI can be appraised at both wavelengths. In the near-infrared, LAI–θ_l reaches its maximum at nadir for those models whereas it is less influential for PROKUUSK. This may explain why the LAD and the LAI are strongly correlated in these viewing configurations during inversion (Jacquemoud, 1993; Qiu, Gao, & Lesht, 1998). The interaction between leaves and soil can be evaluated by means of the LAI–α_{soil} interaction. As expected, the latter is more important in the visible than in the near-infrared because the contrast between canopy and soil reflectances is weaker in the visible. These results give prominence to the interdependence of the parameters when computing bidirectional and spectral reflectances. This issue is particularly important when running a model in the inverse mode: besides the fact that two different combinations of the parameters may give similar reflectance values, making the solution of the inverse problem nonunique, the interactions between parameters may result in slow inversions and inaccurate estimations.

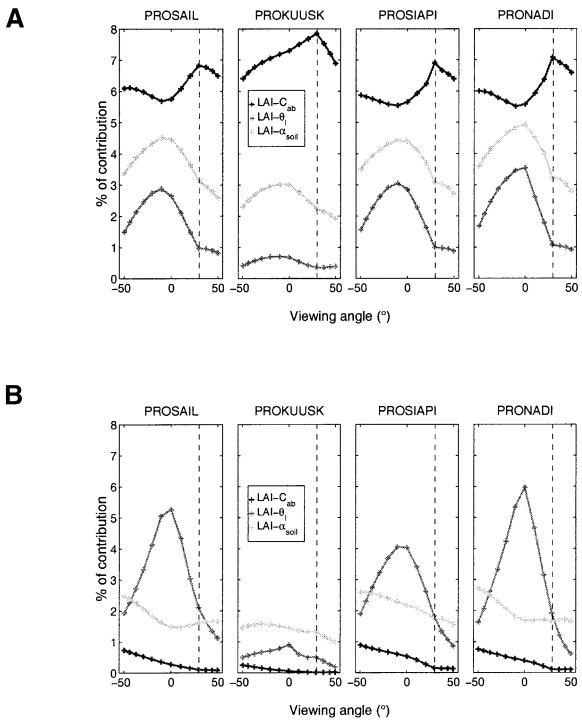

Fig. 8. Contribution of LAI–C_{ab}, LAI–θ_l, and LAI–α_{soil} interactions as a function of the zenith viewing angle at (A) 670 and (B) at 865 nm (the dashed line indicates the solar illumination direction).

4. Conclusion

The design of numerical experiments has proved to be an efficient tool for studying model sensitivity to their input parameters. It has been used to compare four CR models on the basis of a set of 343 simulations leading to 17,836 bidirectional and spectral reflectances, in the four spectral bands and 13 viewing angles of the spaceborne POLDER instrument. The results of PROSAIL, PRONADI, and PROSIAPI, models appear to be coherent while PROKUUSK stands apart. The main discrepancies are attributed to the parameter describing the leaf inclination, as seen when considering the effects of the mean leaf angle. Indeed, the comparisons have been carried out by first assessing the relative influences of N, C_{ab}, LAI, θ_l, s_l, and α_{soil}, and the interactions of LAI–C_{ab}, LAI–θ_l, and LAI–α_{soil} to the reflectance. The relative contribution of θ_l is lower for PROKUUSK when θ_l describes a planophile or an erectophile canopy; the interactions are lower for this model than for PROSAIL, PRONADI, and PROSIAPI. The differences in the leaf inclination parameter effect express different representations of the LAD (elliptical in PROKUUSK, ellipsoidal in the others) and above all,

different implementations of the G and phase functions (especially in PROKUUSK where the analytical approximations used make the model to diverge). Otherwise, for the other input parameters, the models show good agreement both spectrally and directionally. The differences are rather in the magnitude of the parameters' effect than in the general shape of their representative curves.

The method described in this paper to study sensitivity of models improves previous sensitivity analyses insofar as the possibility that factors may interact is accounted for. Also, an important result brought out is the hierarchy of the parameters' contribution to the reflectance. Clearly, the leaf chlorophyll content mainly drives the reflectance in the visible, whereas the LAI and the LAD have the largest contribution to the outputs in the near-infrared. Most of these relationships have been observed for a long time, but they were not explicitly brought to the fore and mathematically quantified. The fact that the influence of LAI and θ_l are of the same magnitude, and that they interact spectrally and directionally, should lead to revise model inversions that fix the LAD during the process, otherwise erroneous values of LAI may be retrieved. Surprisingly, it appears that the simple 1D model, PROSAIL, manages to fit the outputs of more complicated ones. The inversion of these models on more extensive experimental data sets should refine the comparisons, as it is now the prime way to validate a model. Nevertheless, the design of experiment could also be applied to model validations in the direct mode. In particular, it is of primary interest to validate the effects drawn from simulations with results from laboratory experiments where the biophysical parameters of interest would be varied independently from one another, or with a 3D radiative transfer model. Especially for the LAD, which directionally shapes the reflectance of a canopy and spectrally drives its magnitude. In conclusion, the use of experimental designs for model intercomparisons appears both as an objective approach and as a promising option to improve and standardize these studies. The reasons are that (i) the parameter space is better explored (the input variables vary simultaneously in a restricted number of computations), (ii) a wider range of reference canopies is provided, and (iii) the comparisons can also be centered on the input parameters effects and their interactions, which only requires the models' outputs.

Acknowledgments

The authors want to thank N. Gobron (JRC, Ispra, Italy), J. Iaquinta (LAMP, Clermont-Ferrand, France), and A. Kuusk (Tartu Observatory, Estonia) for providing the NADI, IAPI, and KUUSK models, respectively. This work was supported by the Programme National de Télédétection Spatiale (PNTS). In addition, many thanks to A. Kuusk, S. L. Ustin, and S. Flasse for their valuable comments.

References

Asner, G. P. (1998). Biophysical and biochemical sources of variability in canopy reflectance. *Remote Sensing of Environment*, *64*, 234–253.

Benoist, D., Tourbier, Y., & Germain-Tourbier, S. (1994). *Plans d'expériences: construction et analyse*. Paris: Coll. Tec & Doc, Lavoisier (693 pp.).

Bowman, K. P., Sacks, J., & Chang, Y. F. (1993). Design and analysis of numerical experiments. *Journal of Atmospheric Science*, *50* (9), 1267–1278.

Box, G. E. P., Hunter, W. G., & Hunter, J. S. (1978). *Statistics for experimenters: an introduction to design, data analysis and model building*. New York: Wiley (653 pp.).

Campbell, G. S. (1986). Extinction coefficients for radiation in plant canopies calculated using an ellipsoidal inclination angle distribution. *Agricultural and Forest Meteorology*, *36*, 317–321.

Campbell, G. S. (1990). Derivation of an angle density function for canopies with ellipsoidal leaf angle distribution. *Agricultural and Forest Meteorology*, *49*, 173–176.

Church, M., & Lynch, R. O. (1998). Utilizing design of experiments, Monte Carlo simulations and partial least squares in snapback elimination. *Quality and Reliability Engineering International*, *14* (4), 227–235.

Clevers, J. G. P. W., & Verhoef, W. (1991). *Modelling and synergetic use of optical and microwave remote sensing. LAI estimation from canopy reflectance and WDVI: a sensitivity analysis with the SAIL model* (Report 2), in Report 90-39 of the Netherlands Remote Sensing Board (BCRS), 70 pp.

Combal, B., Oshchepkov, S. L., Sinyuk, A., & Isaka, H. (2000). Statistical framework of the inverse problem in retrieval of vegetation parameters. *Agronomy*, *20* (1), 65–77.

Dechambre, M., & Le Gac, Ch. (2001). Comparison of two microwave backscattering models by means of sensitivity study based on an experimental design method. *Remote Sensing of Environment* (submitted).

Deschamps, P.-Y., Bréon, F.-M., Leroy, M., Podaire, A., Bricaud, A., Buriez, J.-C., & Sèze, G. (1994). The POLDER mission: instrument characteristics and scientific objectives. *IEEE Transactions on Geoscience Remote Sensing*, *32* (3), 598–614.

Fisher, R. A. (1925). *Statistical methods for research workers*. London: Oliver & Boyd (239 pp.).

Gobron, N., Pinty, B., Verstraete, M. M., & Govaerts, Y. (1997). A semidiscrete model for the scattering of light by vegetation. *Journal of Geophysical Research, [Atmospheres]*, *102* (D8), 9431–9446.

Goel, N. (1988). Models of vegetation canopy reflectance and their use in estimation of biophysical parameters from reflectance data. *Remote Sensing Review*, *4* (1), 1–222.

Iaquinta, J. (1995). *Champs de rayonnement émergeant des surfaces terrestres: modélisation et inversion dans le cas de milieux optiquement finis et couplés avec une couche atmosphérique.* Thèse de Doctorat, Université Blaise Pascal.

Iaquinta, J., & Pinty, B. (1994). Adaptation of a bidirectional reflectance model including the hot-spot to an optically thin canopy. In: *Proceedings of the 6th International Symposium on Physical Measurements and Signatures in Remote Sensing, Val d'Isère, France, 17–21 January 1994* (pp. 683–690) (Editions du CNES, Toulouse).

Jacquemoud, S. (1993). Inversion of the PROSPECT + SAIL canopy reflectance model from AVIRIS equivalent spectra: theoretical study. *Remote Sensing of Environment*, *44*, 281–292.

Jacquemoud, S., Bacour, C., Palvé, H., & Frangi, J.-P. (2000). Comparison of four radiative transfer models to simulate plant canopies reflectance — direct and inverse mode. *Remote Sensing of Environment*, *74*, 471–481.

Jacquemoud, S., Ustin, S. L., Verdebout, J., Schmuck, G., Andreoli, G., & Hosgood, B. (1996). Estimating leaf biochemistry using the PROSPECT leaf optical properties model. *Remote Sensing of Environment*, *56* (3), 194–202.

Kimes, D. S. (1984). Modeling the directional reflectance from complete

homogeneous vegetation canopies with various leaf-orientation distributions. *Journal of the Optical Society of America A: Optics, Image Science, and Vision*, *1* (7), 725–737.

Kuusk, A. (1985). The hot spot effect of a uniform vegetative cover. *Soviet Journal of Remote Sensing*, *3* (4), 645–658.

Kuusk, A. (1995a). A Markov chain model of canopy reflectance. *Agricultural and Forest Meteorology*, *76*, 221–236.

Kuusk, A. (1995b). A fast, invertible canopy reflectance model. *Remote Sensing of Environment*, *51*, 342–350.

Kuusk, A., Andrieu, B., Chelle, M., & Aries, F. (1997). Validation of a Markov chain canopy reflectance model. *International Journal of Remote Sensing*, *18* (10), 2125–2146.

Myneni, R. B., Maggion, S., Iaquinta, J., Privette, J. L., Gobron, N., Pinty, B., Kimes, D. S., Verstraete, M. M., & Williams, D. L. (1995). Optical remote sensing of vegetation: modeling, caveats, and algorithms. *Remote Sensing of Environment*, *51*, 169–188.

Myneni, R. B., Ross, J., & Asrar, G. (1989). A review on the theory of photon transport in leaf canopies. *Agricultural and Forest Meteorology*, *45, 1–153.*

Pinty, B., Gobron, N., Widlowski, J. L., Gerstl, S. A. W., Verstraete, M. M., Antunes, M., Bacour, C., Gascon, F., Gastellu, J. P., Goel, N., Jacquemoud, S., North, P., Qin, W., & Thompson, R. (2001). The Radiation transfer Model Intercomparison (RAMI) exercise. *Journal of Geophysical Research, [Atmospheres]*, *106* (11), 11937–11956.

Privette, J. L., Myneni, R. B., Emery, W. J., & Hall, F. G. (1996). Optimal sampling conditions for estimating grassland parameters via reflectance model inversions. *IEEE Transactions on Geoscience Remote Sensing*, *34* (1), 272–284.

Qiu, J., Gao, W., & Lesht, B. M. (1998). Inverting optical reflectance to estimate surface properties of vegetation canopies. *International Journal of Remote Sensing*, *19* (4), 641–656.

Saltelli, A. (1999). Sensitivity analysis: could better methods be used? *Journal of Geophysical Research*, *104* (D3), 3789–3793.

Spuzic, S., Zec, M., Abhary, K., Ghomashchi, R., & Reid, I. (1997). Fractional design of experiments applied to a wear simulation. *Wear*, *212* (1), 131–139.

Verhoef, W. (1984). Light scattering by leaf layers with application to canopy reflectance modeling: the SAIL model. *Remote Sensing of Environment*, *16*, 125–141.

Verhoef, W. (1985). Earth observation modeling based on layer scattering matrices. *Remote Sensing of Environment*, *17*, 165–178.

Verstraete, M. M., Pinty, B., & Dickinson, R. E. (1990). A physical model of the bidirectional reflectance of vegetation canopies: 1. Theory. *Journal of Geophysical Research*, *[Atmospheres]*, *95* (11), 765–775.